

## Removal of heavy metals by immobilized magnetite nano-particles

Adva Zach-Maor, Raphael Semiat, Hilla Shemer\*

*Rabin Desalination Laboratory, Grand Water Research Institute, Department of Chemical Engineering, Technion, Haifa 32000, Israel  
Tel. +972 (4) 8292488; Fax +972 (4) 8292850; email: shilla@tx.technion.ac.il*

Received 11 October 2010; Accepted 6 December 2010

---

### ABSTRACT

Nano-sized magnetite homogenous porous layer was immobilized onto modified granular activated carbon and used as an adsorbent for copper (Cu(II)) and chromium (Cr(VI)). Batch adsorption experiments revealed high efficiency for both metals removal attaining maximum adsorption capacity of 590 mg/g Fe. Significant difference in the reaction kinetics was found between the two metals suggesting that the magnetite affinity towards the copper was much higher than for chromium. These results were explained by the different mechanism at which the metals were adsorbed by the immobilized magnetite nano-particles layer. It was concluded that initially the metals were adsorbed by the active sites on the magnetite surface, and then diffused into the interior pores of the nano-magnetite layer. It was demonstrated that the latter was the rate-determining step for the process. Fixed-bed continuous experiments revealed the potential to reuse the nFe-GAC through three consecutive sorption and desorption cycles of copper.

*Keywords:* Activated carbon; Adsorption; Copper; Hexavalent chromium; Iron oxide

---

### 1. Introduction

Heavy metals are among the priority pollutants, as they are non-biodegradable, and often accumulate in the environment causing both short term and long term adverse effects [1]. Both Cr(VI) and Cu(II) are present in effluents of large number of industries. Copper pollution arises from copper mining and smelting, brass manufacture, electroplating, industries and excessive use of Cu-based agri-chemicals. Copper along with arsenic and mercury, is recognized as the highest relative mammalian toxic species. Copper sulfate is widely used as algicide in ornamental ponds and even in water supply reservoirs, which are affected by blooms of blue-green alga [2]. Industrial effluents which contain chromium species in high quantities arise from tanning, electroplating, paint and

textile industries. Even though both trivalent and hexavalent forms of chromium exist in industrial wastewater, the hexavalent form is considered more hazardous due to its carcinogenic properties [3]. Both Cr(VI) and Cu(II) are within the European community list of 13 elements of highest concern, hence their removal from water and wastewater is of major importance.

The conventional methods for heavy metals removal from aqueous solutions include oxidation, reduction, precipitation, membrane filtration, ion exchange, electro-deposition and adsorption [2]. Chemical precipitation and reduction processes require additional separation step for complete removal and disposal of high quantities of metal sludge. These techniques use great deal of chemicals and the residual heavy metals concentration in the treated water is not always achieving the regulations guidelines. The application of membrane system for wastewater treatment has major problems such as

---

\* Corresponding author.

membrane scaling, fouling and blocking. The drawback of the ion exchange process is the high cost of resin while the electro-deposition method is more energy intensive than other methods [3]. Among these methods adsorption is one of the most promising technologies, as high removal efficiencies can be reached when using proper sorbents [1]. Adsorption of trace heavy metals onto solid phases and associated surface coatings is considered very important in controlling heavy metal activity. In recent years considerable attention has been paid to the investigation of different types of adsorbents especially using metal-oxide modified adsorbents, such as sand [2], zeolite [4], diatomite [5] and activated carbon [6]. Adsorption of trace heavy metals is expected to be governed by the composition of solid phases and in particular the content of metal oxides. Iron oxides are considered important sorbents for trace heavy metals therefore, they have been studied extensively. Moreover, varying commercial ferric hydroxide sorbents showed promising results for removal of heavy metals [1].

Adsorption processes could be enhanced by extending adsorbent surface area. Therefore, by reducing iron oxides particles size (i.e., increasing their surface area) enhanced sorption is expected. However, small sized nanoparticles may not be separated from aqueous solutions by gravitational sedimentation. Hence, immobilizing the nano-adsorbents onto supporting materials should enable efficient usage of the nano-particles. [7].

The objective of this study was to investigate the removal of copper and chromium by magnetite impregnated granular activated carbon (nFe-GAC). The removal efficiency was compared with virgin granular activated carbon. Adsorption isotherms, kinetics and mechanism are discussed. Reuse of the nFe-GAC is presented.

## 2. Experimental

### 2.1. Materials

Charcoal activated granulated carbon (pure) particle size: 0.5–1.6 mm and potassium dichromate ( $K_2Cr_2O_7$ ) were supplied by Riedel de Haën (Germany); copper (II)

chloride dehydrate ( $CuCl_2 \cdot 2H_2O$ ) from Acros Organics (USA). All chemicals were used as received and all solutions were prepared with de-ionized (DI) water.

### 2.2. Adsorbent preparation

Charcoal granular activated carbon (GAC) was modified using potassium permanganate and impregnated with ferric chloride solution (0.18 M) at a ratio of 20 mL iron solution per 1 g GAC for 2 h at 25°C. The major characteristics of the virgin, modified and iron impregnated carbons are given in Table 1.

### 2.3. Batch adsorption

Batch adsorption tests were conducted using 0.5 g nFe-GAC and virgin carbon and 25 mL of aqueous metal solution (Cu(II) or Cr(VI)) at varying concentrations ranging from 100 to 500 mg/L. Samples were mixed in a water bath (200 rpm) for up to 24 h at 25°C. At regular time intervals an aliquot of supernatant was sampled and the metal concentration was measured. Copper was analyzed using ContrAA®700 flame atomic absorbance (Analytik Jena, Germany) calibrated with ICP multi-element IV standard solution Merck (Germany). Chromium concentration was measured by HACH DR2800 spectrophotometer using ChromaVer®3 Reagent powder pillows (method 8023 with detection limit of 0.010 mg/L  $Cr^{6+}$ ).

Adsorption isotherms were obtained by mixing nFe-GAC (5–30 g/L) with 30 mL of 500 mg/L copper or chromium aqueous solution for 3.5 and 24 h respectively, at 25°C and 200 rpm.

The metal capacity of the GAC was calculated by the following equation:

$$q_{\text{metal}} = \frac{V(C_0 - C_t)}{M_{\text{Fe}}} \quad (1)$$

where  $q_{\text{metal}}$  is the adsorbed copper or chromium (mg/g);  $V$  is the volume of the metal solution (L);  $C_0$  and  $C_t$  are the metal initial and final concentrations respectively (mg/L);  $M_{\text{Fe}}$  is the mass of iron immobilized onto the GAC (g).

Each experiment was repeated in duplicates. Control experiments were conducted at the same procedure

Table 1  
Characteristics of the virgin, modified and magnetite loaded carbons

GAC type	BET surface area (m <sup>2</sup> /g)	Iron capacity (mg Fe/g GAC)	Iron specie	pH <sub>pzc</sub> *
Virgin	1454	14±2.2	—	7.4
Modified	866	—	—	9.2
nFe	1024	33.9±3.6	Fe <sub>3</sub> O <sub>4</sub>	6.9

\*pH<sub>pzc</sub> is the point of zero charge; the pH at which the net surface charge on the adsorbent surface is zero

described above using modified carbon (i.e.,  $\text{KMnO}_4$  pre-treated without iron impregnation).

#### 2.4. Fixed bed adsorption

Fixed bed experiments were conducted using a glass column 25×2.5 cm (i.d.) packed with 2 g nFe-GAC. Copper aqueous solution at initial concentration of 100 mg/L (pH 5.6) was fed to the column in a down-flow mode at a rate of 30 BV/h (corresponding to 4 mL/min) using a peristaltic pump. The column loading was immediately followed by acid regeneration (0.05 M HCl for 30 min) in up-flow mode and a close-loop configuration, at a rate of 250 mL/min resulting in approximately 50% bed expansion. Following the acid recirculation the nFe-GAC was washed with DI water until the pH of the effluent water reached 4. Three cycles of loading/regeneration were applied. The total adsorbed copper quantity (maximum column capacity) was calculated by integrating the copper adsorbed concentration vs. the throughput volume [Eq. (2)].

$$q_{\text{copper}} = \int_0^{V_T} \frac{(C_0 - C_t) dV}{M_{\text{Fe}}} \quad (2)$$

where  $V_T$  is the volume of effluent collected upon exhaustion of the bed;  $C_0$  and  $C_t$  are the copper initial and effluent concentrations respectively (mg/L);  $M_{\text{Fe}}$  is the mass of iron immobilized onto the GAC (g).

### 3. Results and discussion

Homogenous layer of nano-sized magnetite particles (<4 nm) was synthesized by impregnation of modified granular activated carbon with ferric chloride. A significant increase in the surface area of the matrix following iron loading (Table 1), indicated that a porous nano-magnetite layer was formed. Detailed description of the synthesis conditions and mechanism of magnetite formation as well as nFe-GAC characterization is specified elsewhere [8].

#### 3.1. Adsorption of chromium and copper

Removal of copper (Cu(II)) and hexavalent chromium (Cr(VI)) by virgin, modified and magnetite loaded carbons were investigated. One of the methods used for removal of inorganic pollutants from pollutant water is adsorption by activated carbon. Therefore, the removal of the studied heavy metals by the synthesized nFe-GAC was compared with untreated activated carbon (virgin). Results indicated higher adsorption capacities by the nFe-GAC compared with the virgin carbon. For example, 68% and 91% of chromium (at initial concentration of 100 mg/L) were removed by the virgin and nFe-GAC carbons respectively after 4 h (Fig. 1). Copper adsorption (at initial concentration of 500 mg/L) followed the same

pattern where, 32% and 85% were removed by the virgin and nFe-GAC carbons respectively after 6 h (Fig. 2).

The adsorption of chromium and copper by the nFe-GAC followed two steps. A fast initial sorption followed by much slower adsorption process (Figs. 1 and 2). This two step differential adsorption rates, which can last hours and even days is characteristic to adsorption onto iron oxides [9].

Adsorption studies for copper were carried out at three initial concentrations of 100, 250, and 500 mg/L due to the extremely high adsorption capacity of nFe-GAC, as illustrated in Fig. 2. For concentrations lower than 500 mg/L it is clear that adsorption limiting factor was the copper concentration as for  $C/C_0$  reduces to zero within 4 h. Only at initial concentration of 500 mg/L copper was measurable at  $t > 4$  h.

In order to truly evaluate the role of magnetite nanoparticles in the adsorption of the heavy metals, modified GAC (i.e., without iron loading) was tested for Cu and Cr removal. As can be seen from Fig. 1, results indicated that the modified GAC was inert to the chromium adsorption process. Sorption of copper by the modified GAC could not be determined since at pH > 6 precipitation of insoluble copper hydroxides ( $\text{Cu}(\text{OH})_2$ ) occurs [10–12]. The modified carbon is alkaline with  $\text{pH}_{\text{PZC}}$  of 9.2 (Table 1) hence immediate precipitation of copper was obtained once the modified carbon was mixed with aqueous copper solution.

#### 3.2. Adsorption kinetics models

The kinetics of the adsorption processes was characterized in terms of reaction rate and mechanism (mass transfer and/or diffusion control reaction). The experimental data was fitted with the linearized form of three kinetic models including: pseudo first order Eq. (3)

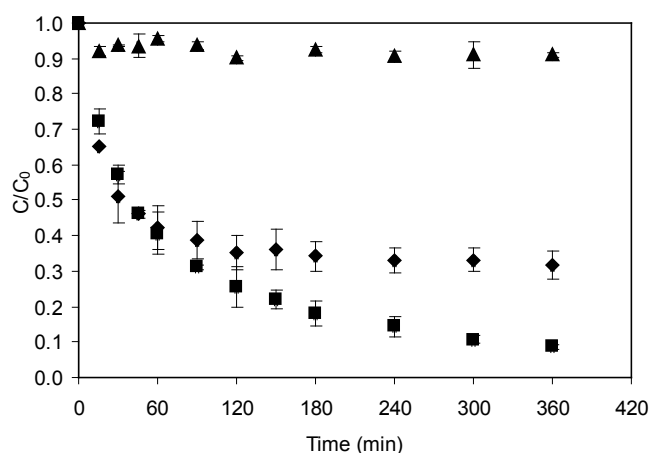


Fig. 1. Chromium adsorption by (▲) pre-treated, (◆) virgin and (■) nFe-GAC carbons with time at initial concentration of 100 mg/L and temperature of 25°C.

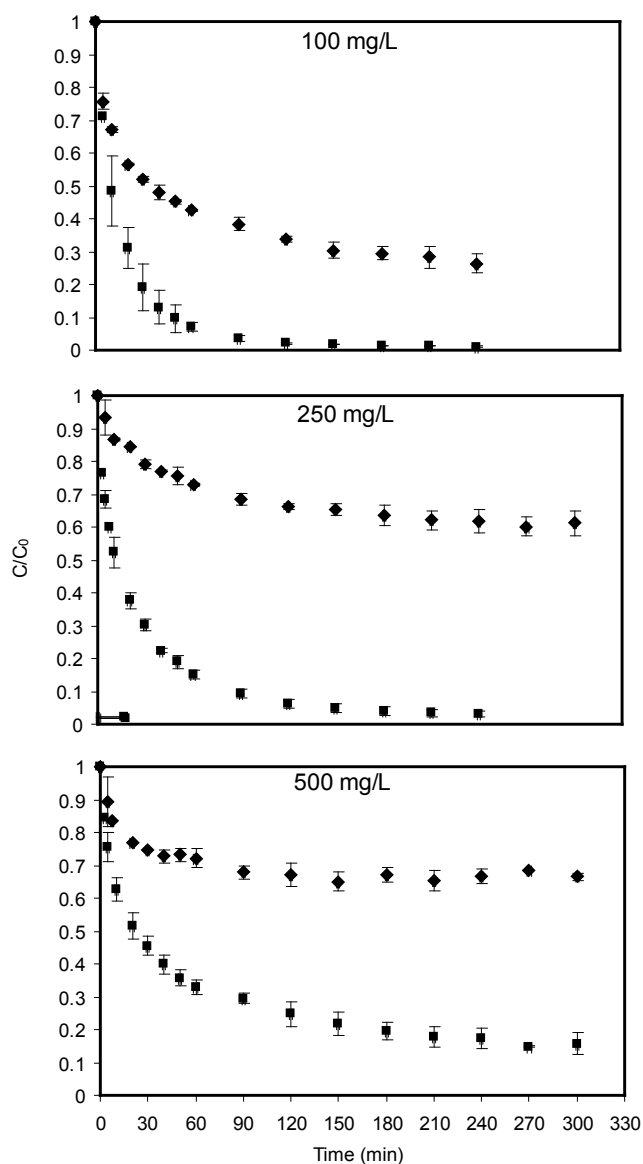


Fig. 2. Copper adsorption by (♦) virgin and (■) nFe-GAC carbons with time at varying initial concentrations ranging from 100 to 500 mg/L at 25°C.

pseudo second order Eq. (4), and intra-particle diffusion Eq. (5) [13,14].

$$\log(q_e - q_t) = \log q_e - \frac{k_1}{2.303} t \quad (3)$$

$$\frac{t}{q_t} = \frac{1}{k_2 q_e^2} + \frac{1}{q_e} t \quad (4)$$

$$q_t = K_{int} t^{0.5} \quad (5)$$

where  $k_1$  (1/min) and  $k_2$  (mg/g min) are the first order and second order rate constants of adsorption respectively,  $q_e$  (mg/g) is the equilibrium adsorption capacity,  $q_t$  (mg/g)

is the adsorption at time  $t$  (min), and  $K_{int}$  is the intra particle diffusion constant (mg/g min<sup>0.5</sup>). All the kinetic parameters, other than  $K_{int}$ , were determined from the slopes and the intercepts of respective plots and are summarized in Table 2.

Contaminants adsorption onto the nFe-GAC was best described by the pseudo-second order model for both metals tested, as shown in Fig. 3A ( $r^2 \approx 1.0$ ). Whereas, the pseudo-first order exhibited very low correlation coefficients (Table 2).

Intra-particle diffusion/ transport process is often regarded as the rate limiting step of adsorption processes. Intra-particle diffusion constants were calculated by plotting  $q_t$  vs.  $t^{0.5}$  (Fig. 3B). As seen in the figure, two separate regions were obtained exhibiting different slopes, indicating multistep limited adsorption process. The intra particle diffusion adsorption is controlled by the diffusion of ions within the adsorbent. Generally, the initial steep slope of the plot (region I) relates to the film diffusion and the latter moderate slope (region II) represents the diffusion within the adsorbent. When taking into account the current adsorbent structure, it could be postulated that the different adsorption rates are attributed to fast

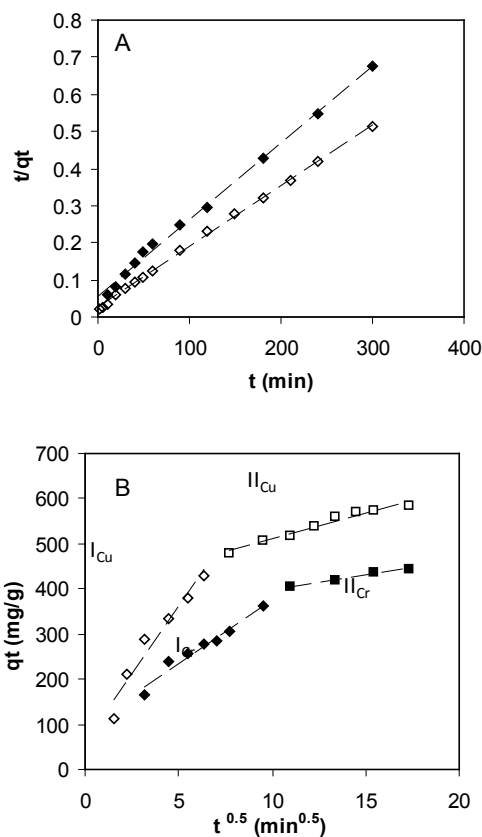


Fig. 3. Adsorption kinetics of Cu(II) (♦) and Cr(VI) (♦) onto nFe-GAC analyzed by pseudo-second (A) and intra-particle diffusion models (B). Initial concentrations of both metals 500 mg/L at 25°C.

Table 2

Kinetics parameters for Cu(II) and Cr(VI) adsorption on nFe-GAC, initial concentrations of both metals 500 mg/L at 25°C

Metal	$q_e$ (mg/g)	Pseudo first order			Pseudo second order			Intra-particle diffusion	
		$q_1$ (mg/g)	$k_1$ (1/min)×10 <sup>2</sup>	$r^2$	$q_2$ (mg/g)	$k_2$ (g/mg min)×10 <sup>3</sup>	$r^2$	* $k_{int}$ (g/g min <sup>0.5</sup> )	$r^2$
Cu	576.4	330.4	1.38	0.927	625.0	0.104	0.999	12.4	0.965
Cr	444.1	352.0	0.37	0.888	476.2	0.078	0.997	6.58	0.986

\*Obtained from the slope of region II in Fig. 3B

sorption onto the magnetite surface (region I) followed by diffusion into the porous layer which is a much slower process (region II). Therefore, it can be concluded that the metals adsorption process is governed by diffusion within the nano-metric porous structure [8]. These results correspond well with published literature concerning the kinetics of trace metals on iron oxides crystals. It was suggested that the process involved rapid adsorption on the external surface of the crystals followed by slow diffusion into the particles, and finally adsorption on internal sites. The latter step may continue over days [9]. When comparing nFe-GAC adsorption performance towards the two metals, it could be clearly seen (Table 2) that the rate constant is much higher for copper. This is further elucidated when analyzing the intra-particle diffusion plots (Fig. 3B); here it is obvious that the initial adsorption step (i.e. onto the magnetite nano-particles surface) is much faster for copper than for chromium. Moreover, the adsorption capacity of the nFe-GAC is higher for Cu(II), as the absolute  $q_i$  values are clearly higher than for Cr(VI).

### 3.3. Adsorption isotherms

The relationship between adsorbed ion concentration and its concentration in the solution at equilibrium is described by isotherm models. The sorption data was described using the Langmuir and Freundlich isotherms which are the most widely used models, shown in Eqs. (6) and (7) [14, 15].

$$q_e = q_m \frac{bC_e}{1 + bC_e} \quad (6)$$

$$q_e = K_f C_e^{1/n} \quad (7)$$

where  $q_e$  is the equilibrium adsorption capacity (mg/g),  $C_e$  is the equilibrium concentration of solution (mg/L),  $b$  is the Langmuir constant related to the energy of adsorption (L/mg) and  $q_m$  is the maximum adsorption capacity (mg/g). The values of Langmuir constants  $q_m$  and  $b$  were obtained from the intercept and slope of the linear plot of  $C_e/q_e$  vs.  $C_e$  (Eq.6).  $K_f$  and  $n$  are constants for Freundlich isotherm that are indicative of adsorption capacity (mg/g) and intensity of the adsorbent respectively [16].

Table 3

Isotherm constants for adsorption of Cu(II) and Cr(VI) onto nFe-GAC. Initial concentrations of both metals 500 mg/L; equilibrium time 3.5 and 24 h for Cu and Cr respectively

	Langmuir			Freundlich		
	$b$ (L/mg)	$q_m$ (mg/g)	$r^2$	$n$	$K_f$ (mg/g)	$r^2$
Cu	0.020	588	0.988	3.6	95.8	0.985
Cr	0.017	588	0.973	2.8	61.2	0.953

The values of  $K_f$  and  $n$  were calculated from the slope and intercept of the plot generated from the logarithmic form of Eq. (7) [17]. The calculated constants are reported in Table 3.

Equilibrium time was defined as the time required to remove ≥80% of the metal initial concentration, although 100% removal is expected after infinite time. As kinetic analysis revealed chromium adsorption was much slower than copper (its reaction rate constant is an order of mag-

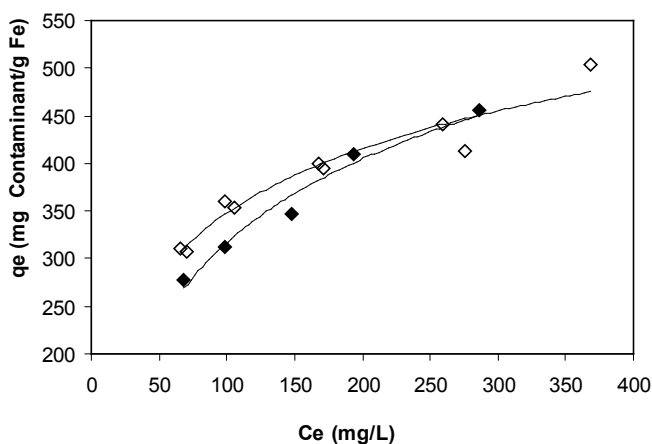


Fig. 4. Adsorption isotherm of Cu (◇) and Cr (◆) by nFe-GAC at 25°C. Initial concentrations of both metals 500 mg/L; equilibrium time 3.5 and 24 h for Cu(II) and Cr(VI) respectively. nFe-GAC concentration ranging from 5 to 30 g/L.

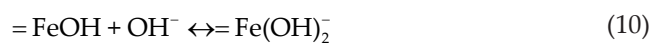
nitude higher). Therefore, the experiments carried out to determine the adsorption isotherms lasted 24 h for Cr(VI) and only 3.5 h for Cu(II).

Inspection of the regression coefficients revealed that Langmuir model, shown in Fig. 4, best described the experimental data for both metals as compared with the Freundlich model. Langmuir isotherm model represent monolayer adsorption occurring on an energetically uniform surface on which the adsorbed molecules are not interactive. Thus, equilibrium is attained once the monolayer is completely saturated [18].

Using the Langmuir model, the maximum sorption capacity for the metals was estimated at 588 mg/g Fe for both copper and chromium. However, the significant difference in reaction kinetics suggests that nFe-GAC affinity towards copper was much higher than for chromium, as for the same maximum adsorption capacity was reached after only 15% of the time. These results can be further explained by the different mechanisms at which these metals are adsorbed onto the immobilized magnetite nano-particles layer. A detailed discussion regarding the adsorption mechanism of both metals is present herein.

### 3.4. Mechanism of adsorption

In aqueous medium iron oxides can undergo protonation or deprotonation of the –OH groups as follows [19]:

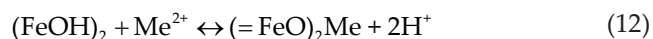


The surface charge at the iron-oxide/H<sub>2</sub>O interface depends on the pH of the solution. The p*H*<sub>PZC</sub> of the synthesized nFe-GAC is near natural pH at 6.9 (Table 1) hence, it can be used as an adsorbent of both positively and negatively charged metals.

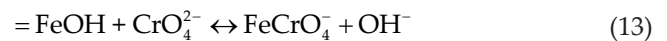
The specific adsorption of divalent metal cation (Me<sup>2+</sup>), such as copper, at the iron-oxide/H<sub>2</sub>O interface was described as metal ion complexation with a release of a proton [19]:



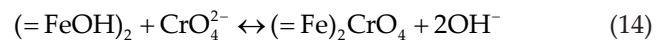
and



Inorganic anions, such as chromium, replace the surface –OH groups thus forming inner-sphere surface complexes [19]. At pH ranging from 1.0 to 6.0 chromium species such as Cr<sub>2</sub>O<sub>7</sub><sup>2-</sup>, HCrO<sub>4</sub><sup>-</sup>, Cr<sub>3</sub>O<sub>10</sub><sup>2-</sup>, Cr<sub>4</sub>O<sub>13</sub><sup>2-</sup> coexist, at which HCrO<sub>4</sub><sup>-</sup> predominates. As the pH increases this latter form shifts to CrO<sub>4</sub><sup>2-</sup> and Cr<sub>2</sub>O<sub>7</sub><sup>2-</sup> [3]. Experiment were conducted at pH of 5.9 hence, chromium may form the following inner-sphere surface complexes:



and



or



and



Oxide surfaces may also bind soluble metal–ligand (MeL) complexes. In some cases a single adsorbate ion may bind to two or more surface sites (multidentate binding) [19].

### 3.5. Fixed bed adsorption

The potential to reuse the nFe-GAC was studied through fixed bed column experiments. Copper uptake capacity of 487±11 mg Cu/g Fe, as calculated by Eq. (2), was obtained following a single loading cycle. These results agree quite well with the theoretical maximum sorption capacity (588 mg Cu/g Fe) calculated using the Langmuir adsorption model (taking into account the fact that equilibrium is not attained in fixed-bed operation).

Copper breakthrough behavior for the nFe-GAC during three regeneration cycles is illustrated in Fig. 5A. The second and third adsorption cycles were followed by 100% desorption of the loaded copper using HCl (as described in the Experimental section). The copper regeneration efficiency decreased in the second cycle to 65%, yet the same efficiency was obtained in the third cycle.

The regeneration efficiency was calculated using following equation:

$$\text{Regeneration (\%)} = \frac{q_r}{q_0} \times 100 \quad (17)$$

here *q<sub>r</sub>* is the adsorption capacity of the regenerated nFe-GAC and *q<sub>0</sub>* is the capacity after the first cycle.

Reduction in uptake capacity as the cycles proceed is primarily attributes to gradual deterioration of the adsorbent with continuous usage as well as to difficult accessibility to the binding sites. The adsorption capacity also strongly depended on the prior desorption since prolonged elution may destroy the binding sites [20]. Since the copper uptake capacity in the second and third cycles was similar it was proposed that the low pH of the adsorbent following the acidic regeneration caused the reduction in the uptake capacity in the second and third cycles. In order to test this hypothesis HCl was re-circulate at the same conditions as the regeneration step prior to the first loading. As seen in Figs. 5A and 5B, the same uptake capacity of copper by the nFe-GAC was observed in the second cycle and following HCl recirculation. These

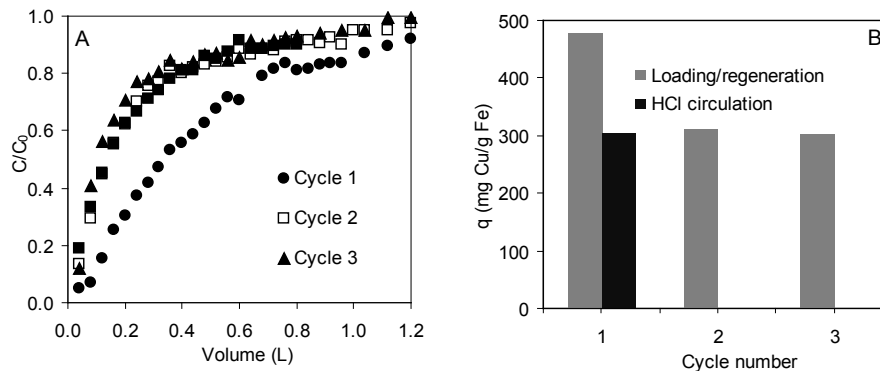


Fig. 5. Breakthrough curves (A) and uptake capacity (B) of copper by nFe-GAC during three regeneration cycles and following recirculation of HCl prior to copper loading (initial concentration of 100 mg/L, pH = 5.6, and 25°C).

results suggest that the pH affected the uptake capacity rather than damage to the adsorbent. It is well established that copper adsorption decreases with increased acidity due to the competition between  $\text{Cu}^{2+}$  ions and  $\text{H}^+$  ions for the same sites. At higher pH the adsorption of  $\text{Cu}^{2+}$  is high due to the attraction between the negatively charged surface of an adsorbent and the metal [10–12].

## References

- [1] H. Genç-Fuhrman, P. Wu, Y. Zhou and A. Ledin, Removal of As, Cd, Cr, Cu, Ni and Zn from polluted water using an iron based sorbent, *Desalination*, 226 (2008) 357–370.
- [2] N. Boujelban, J. Bouzid and Z. Elouear, Adsorption of nickel and copper onto natural iron oxide-coated sand from aqueous solutions: Study in single and binary systems, *J. Hazard. Mater.*, 163 (2009) 376–382.
- [3] T. Karthikeyan, S. Rajgopal and L.R. Miranda, Chromium (VI) adsorption from aqueous solution by *Hevea brasiliensis* sawdust activated carbon, *J. Hazard. Mater.*, 124 (2005) 192–199.
- [4] R.H. Han, W. Zou, Z.P. Zhang, J. Shi and J.J. Yang, Kinetic study of adsorption of Cu(II) and Pb(II) from aqueous solutions using manganese oxide coated zeolite in batch mode, *Colloid Surf. A: Phys. Eng. Asp.*, 279 (2006) 238–246.
- [5] A.M. Khaisheh Majeda, S. Al-Degs Yahya and A.M. McMinn, Remediation of wastewater containing heavy metals using raw and modified diatomite, *Chem. Eng. J.* 99(2) (2004) 177–184.
- [6] N. Zhang, L.S. Lin and D. Gang, Adsorptive selenite removal from water using iron-coated GAC adsorbents, *Wat. Res.*, 42 (2008) 3809–3816.
- [7] C. Xu and A.S. Teja, Characteristics of iron oxide/activated carbon nanocomposites prepared using supercritical water, *Appl. Catal. A: General*, 348 (2008) 251–256.
- [8] A. Zach-Maor, R. Semiat and H. Shemer, Synthesis, performance and modeling of immobilized nano-sized magnetite layer for phosphate removal, *J. Colloid Interf. Sci.*, in press.
- [9] R.M. Cornell and U. Schwertmann, *The Iron Oxides: Structure, Properties, Reactions, Occurrences and Uses*, Wiley VCH, New York, 2003.
- [10] O. Gok, A. Ozcan, B. Erdem and A. Safa Ozcan, Prediction of the kinetics, equilibrium and thermodynamic parameters of adsorption of copper(II) ions onto 8-hydroxy quinoline immobilized bentonite, *Colloid Surf. A: Phys. Eng. Asp.*, 317 (2008) 174–185.
- [11] G.Z. Kyzas, M. Kostoglou and N.K. Lazaridis, Copper and chromium(VI) removal by chitosan derivatives—Equilibrium and kinetic studies, *Chem. Eng. J.* 152 (2009) 440–448.
- [12] M.H. Kalavathy and L.R. Miranda, Comparison of copper adsorption from aqueous solution using modified and unmodified *Hevea brasiliensis* saw dust, *Desalination*, 225 (2010) 165–174.
- [13] M. Özacar, Contact time optimization of two-stage adsorber design using second-order kinetic model for the adsorption of phosphate onto alunite, *J. Hazard. Mater.*, 137 (2006) 218–225.
- [14] Y.A. Adyin and N.D. Aksoy, Adsorption of chromium on chitosan: Optimization, kinetics and thermodynamics, *Chem. Eng. J.*, 151 (2009) 188–194.
- [15] Z. Gu, J. Fang and B. Deng, Preparation and evaluation of GAC-based iron-containing adsorbents for arsenic removal, *Environ. Sci. Technol.*, 39 (2005) 3833–3843.
- [16] S.P. Dubey and K. Gopal, Adsorption of chromium (VI) on low-cost adsorbents derived from agricultural waste material: A comparative Isotherm study, *J. Hazard. Mater.*, 145 (2007) 465–470.
- [17] T.S. Anirudhan and P.G. Radhakrishnan, Kinetic and equilibrium modeling of cadmium(II) ions sorption onto polymerized tamarind fruit shell, *Desalination*, 249 (2009) 1298–1307.
- [18] S. Musić and M. Ristić, Adsorption of trace elements or radionuclides on hydrous iron oxides, *J. Radioanal. Nucl. Chem.*, 120 (1988) 289–304.
- [19] H. Kalavathy, B. Karthik and L.R. Miranda, Removal and recovery of Ni and Zn from aqueous solution using activated carbon from *Hevea brasiliensis*: Batch and column studies, *Colloids Surf B Biointerfaces.*, 78 (2010) 291–302.